WEAK BUMP QUASARS

NASA Grant NAG5-1771

FINAL REPORT

For the Period 15 September 1991 through 14 December 1993

Principal Investigators
Dr. B.J. Wilkes/Dr. J. McDowell

January 1994

Prepared for:

National Aeronautics and Space Administration
Goddard Space Flight Center
Greenbelt, Maryland 20771

Smithsonian Institution
Astrophysical Observatory
Cambridge, Massachusetts 02138

The Smithsonian Astrophysical Observatory
is a member of the
Harvard-Smithsonian Center for Astrophysics

The NASA Technical Officer for this grant is Dr. Robert Petre, Code 666, Laboratory for High Energy Astrophysics, Space Sciences Directorate, Goddard Space Flight Center, Greenbelt, MD 20771.

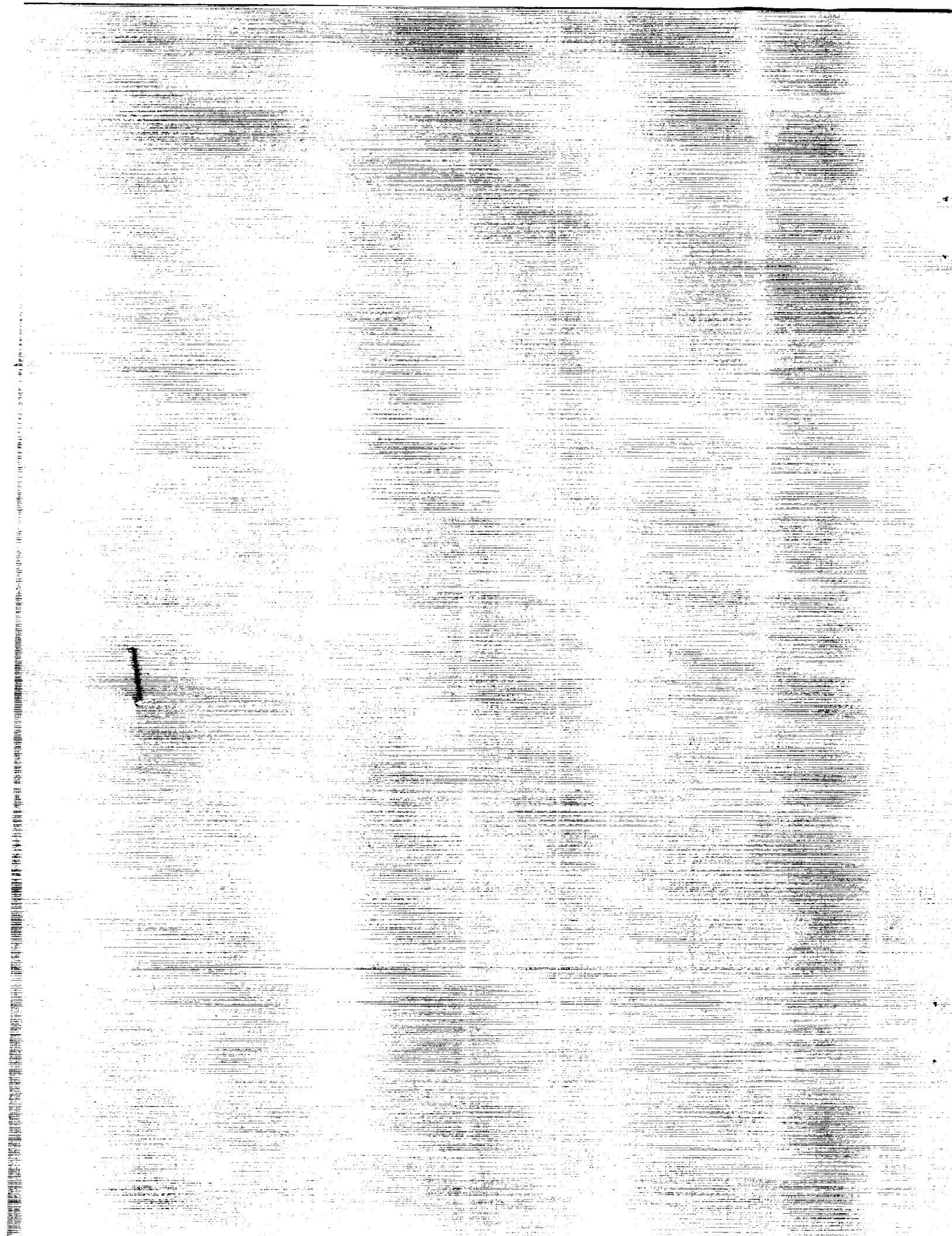

In this investigation I have carried out research into the optical, ultraviolet and infrared continuum emission from quasars and their host galaxies. The main results have been the discovery of quasars with unusually weak infrared emission and the construction of a quantitative estimate of the dispersion in quasar continuum properties.

One of the major uncertainties in the measurement of quasar continuum strength is the contribution to the continuum of the quasar host galaxy as a function of wavelength. Continuum templates have been constructed for different types of host galaxy and individual estimates made of the decomposed quasar and host continua based on existing observations of the target quasars. The results are that host galaxy contamination is worse than previously suspected, and some apparent weak bump quasars are really normal quasars with strong host galaxies. However we have confirmed the existence of true weak bump quasars such as PHL 909.

The study of the link between the bump strength and other wavebands has been continued by comparing with IRAS data. There is evidence that excess far infrared radiation is correlated with weaker ultraviolet bumps. This argues against an orientation effect and implies a probable link with the host galaxy environment, for instance the presence of a luminous starburst. However the evidence still favours the idea that reddening is not important in those objects with ultraviolet weak bumps.

The same work has led to the discovery of a class of infrared weak quasars. Pushing another part of the envelope of quasar continuum parameter space, the IR-weak quasars have implications for understanding the effects of reddening internal to the quasars, the reality of ultraviolet turnovers, and may allow further tests of the Phinney dust model for the IR continuum. They will also be important objects for studying the claimed IR to x-ray continuum correlation.

With the opening of the ROSAT public archive we have been able to extract a set of quasars and carry out spectral fits to extend our x-ray sample size. We have been able to extract from the NDADS archive and reduce fifty more IUE exposures of our target

quasars. Our paper on quasar energy distributions is now ready for submission to the Ap.J. Supplement Series and we have begun a second paper which will summarize the results from the work done on this grant. We are preparing to revise the energy distribution database software package to make it available to the community. To this end we are developing a standard format for multiwaveband energy distribution data which will be compatible with the new FITS BINTABLE standard whose IAU approval is pending.

I have prototyped a new FITS BINTABLE format which will allow a standard way for investigators to record multiwaveband data of the kind studied here.

Poster papers on the above work have been presented at the following conferences:

Testing the AGN Paradigm (AIP Conference Proceedings 254, 1992, p.532)

179th AAS Meeting (Bull. AAS, 23, 4, 1991 p. 1424)

2nd New England Regional Quasar/AGN Meeting (1992, unpublished).

1st IoA-IAP-Leiden Conference, Cambridge, England July 1992.

3rd New England Regional Quasar/AGN Meeting, Cambridge,MA May 1993.

IAU Symposium 159 (1993, in press).

In addition this work has necessitated substantial revision to the "Atlas of Quasar Energy Distributions, Paper I" which is currently undergoing referee-requested revisions and will appear in the Astrophysical Journal Supplement Series. The full results of this investigation will be written up as Paper II in the series.

Appended are the paper from Testing the AGN paradigm and a selection of the results from the Atlas of Quasar Energy Distributions paper.

INFRARED WEAK QUASARS

McDowell, J.C, Elvis, M., and Wilkes, B.J.
Harvard-Smithsonian Center for Astrophysics, Cambridge, MA 02138

ABSTRACT

We present some examples of quasars with anomalously weak infrared emission, and discuss the effects of starlight subtraction on estimates of the ultraviolet and infrared component strengths.

INTRODUCTION

The energy distributions of most quasars (e.g. Neugebauer et al 1987, Sanders et al 1989) have a prominent inflection at about 1.5 microns, where the 'ultraviolet bump' component meets an infrared component. The nature of the infrared component remains unclear. Original suggestions that it was a nonthermal power law have been largely supplanted in recent years by the idea of thermal dust emission. Since the two decade wide infrared component often contains comparable luminosity to the observable decade of the ultraviolet component, this implies that *in at least some directions* a substantial fraction of the bump component is being reprocessed. If the UV all gets out on one axis and is progressively more obscured as one looks towards the plane of an obscuring torus, one might expect an anticorrelation of the observed UV slope and the IR component strength relati[illegible] to the inflection point (or 'baseline IR luminosity', Carleton et al 1987). However, for our sample (Fig. 1., Elvis et al 1992, in preparation) we observe no significant correlation of this kind.

INFRARED WEAK QUASARS

However, we do notice three objects with unusually weak infrared emission. The energy distributions of these quasars are plotted in Fig. 2; it may be seen that although the near IR inflection is present, the rise towards longer wavelengths is abortive and most of the infrared energy distribution lies below the inflection baseline (a horizontal line drawn on the plots through the near IR local minimum in the energy distribution). This is is sharp contrast to the case for most quasars (Sanders et al 1989) where the IR energy above the inflection baseline is comparable to the observed energy in the ultraviolet bump. We note the good agreement between Einstein and Exosat estimates of PG0026+129's power law spectrum, which is typical for radio-quiet quasars, and the very unusual (Wilkes and Elvis 1987) hard x-ray spectrum of the radio-quiet quasar Kaz 102. Barvainis (1990) pointed out the sharp IR cutoff of PG0026+129; however his comparison

of it with PG1358+043 is misleading, since the latter has a perfectly normal value of L_{IR}/L_{Base}.

The third object, PG0844+349, is included as a cautionary note; its energy distribution is rather similar to the first two objects, but it is known to be in a bright host galaxy (Hutchings and Neff 1991). Subtraction of a starlight template (which peaks near 1 micron) from the energy distribution gives colors within the normal envelope for quasars. Measurements of the host galaxy luminosities for PG0026+129 and Kaz 102 suggest that starlight contamination is not important in those objects, a conclusion supported by the fact that their ultraviolet bumps are of normal strength and so unlikely to be diluted by starlight. A fourth quasar, PG1116+215, was missed by IRAS, but ground based 10 and 20 micron observations suggest it may fall in the same category; PHL 658 is another candidate.

The 'ultraviolet bumps' of these infrared weak quasars are normal, and

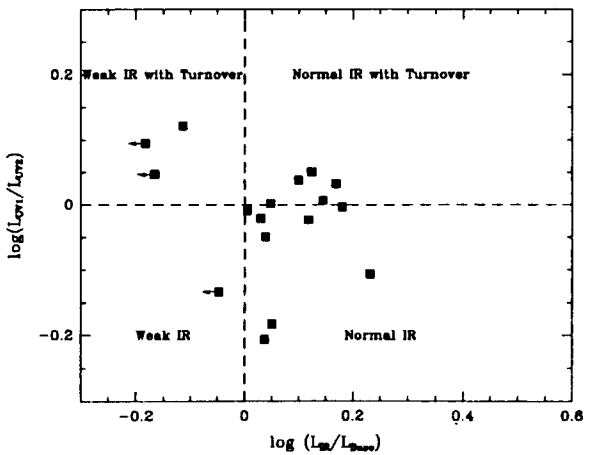

Figure 1: Ultraviolet shape versus infrared strength. The UV shape is determined from the ratio of the continuum flux in two bands in the far UV ($1000 - 2000\mathring{A}$). The IR strength compares the total IR luminosity to the luminosity at the near IR inflection. Data for quasars with both IUE and IRAS data is from Elvis et al (1992).

flatten out in the far UV. If the turnover in these quasars were due to internal reddening, we would expect the energy to be reemitted in the infrared; the lack of infrared emission strongly implies that in these objects the ultraviolet turnover is in fact intrinsic. (The total luminosity of the 1-100 micron region is about 1.2 times the luminosity missing from the observed 2000-1000A region of the spectrum assuming an extrapolation of the 8000-1500A slope; any reasonable extrapolation

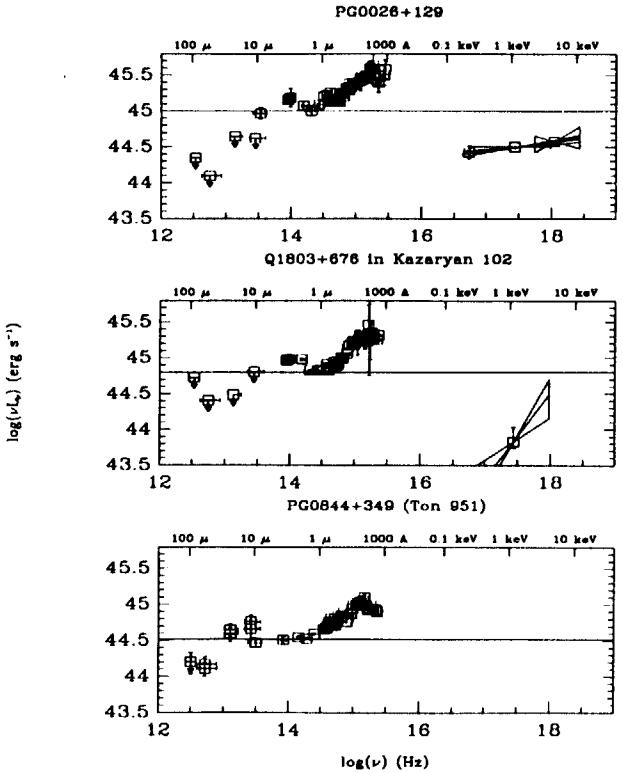

Figure 2: Infrared weak quasars. Plot shows logarithm of energy per unit logarithmic frequency from far infrared to x-ray for three radio-quiet quasars whose infrared emission is unusually weak relative to the optical and ultraviolet. A horizontal line is drawn through the near infrared inflection point to guide the eye.

of the continuum into the unobserved EUV would give missing energy in excess of this total infrared luminosity). We suggest these unusual objects may be suitable candidates for detailed modelling.

DISCUSSION

If we are to test accretion disk models of the quasar continuum, we must be able to compare the models with the observations. Inferred model parameters are very sensitive to the position of the peak of the ultraviolet energy distribution (assumed to represent the disk emission). In many low redshift objects the peak is not seen; even in those objects where the turnover is clear, the concern exists that the turnover may not be intrinsic but instead due to reddening within the quasar host galaxy. Although several lines of argument, most forcefully the low hydrogen columns inferred from x-ray spectral observations, suggest that typical quasars have little line-of-sight reddening, many Seyfert galaxies have a UV continuum that is clearly reddened, and the suggested interpretation of the quasar infrared continuum as emission from dust gives the reddening question renewed importance. The small number of unusual quasars with weak infrared emission will serve as a useful probe of the the quasar phenomenon in the absence of dominant dust reprocessing.

This poster reports work done as part of the Atlas of Quasar Energy Distributions project under NASA grants NAG8-689 and NAGW-2201. JCM acknowledges an NAS/NRC Research Associateship.

REFERENCES

Barvainis, R., 1990. Ap.J., **419**, 432.

Carleton, N.P., Elvis, M., Fabbiano, G., Lawrence, A., Ward, M.J., and Willner, S.P., 1987. Ap J., **318**, 595.

Elvis, M., Wilkes, B., McDowell, J.C., Green, R.F., Bechtold, J., Willner, S.P., Oey, M.S., and Polomski, E., 1992, in preparation.

Hutchings, J., and Neff, S., 1991. A.J. **101**, 434.

Neugebauer, G., Green, R.F., Matthews, K., Schmidt, M., Soifer, B.T. and Bennett, J., 1987. Ap J.Supp., **63**, 615

Sanders, D.B., Sofier, B.T., Elias, J.H., Madore, B.F., Neugebauer, G., and Scoville, N.Z., 1989. Ap J., **347**, 29.

Wilkes and Elvis, 1987. Ap.J., **323**, 343.

TABLE 19
BOLOMETRIC AND MULTIWAVEBAND LUMINOSITIES

Name	UVOIR (0.1 – 100μm)	Bolometric (1 m-10 keV)	Ly cont (912Å-10 keV)	Ionizing Photon Rate
Q0003+158	$46.65^{+0.22}_{-0.12}$	$47.18^{+1.20}_{-0.31}$	$47.01^{+1.35}_{-0.43}$	$46.44^{+0.88}_{-0.25}$
Q0003+199	$45.24^{+0.04}_{-0.05}$	$45.51^{+0.03}_{-0.03}$	$45.14^{+0.01}_{-0.01}$	$44.68^{+0.01}_{-0.01}$
Q0007+106	$45.75^{+0.05}_{-0.05}$	$45.92^{+0.11}_{-0.07}$	$45.34^{+0.21}_{-0.09}$	$44.77^{+0.13}_{-0.08}$
Q0026+129	$45.93^{+0.10}_{-0.12}$	$46.13^{+0.12}_{-0.12}$	$45.66^{+0.10}_{-0.09}$	$45.24^{+0.12}_{-0.12}$
Q0049+171	$44.72^{+0.41}_{-0.10}$	$45.17^{+1.09}_{-0.17}$	$44.98^{+1.25}_{-0.21}$	$44.28^{+1.01}_{-0.17}$
Q0050+124	$46.00^{+0.03}_{-0.03}$	$46.10^{+0.30}_{-0.08}$	$45.32^{+0.82}_{-0.34}$	$44.69^{+0.59}_{-0.22}$
Q0052+251	$46.07^{+0.07}_{-0.07}$	$46.36^{+0.39}_{-0.16}$	$46.00^{+0.62}_{-0.25}$	$45.64^{+0.45}_{-0.23}$
Q0054+144	$46.09^{+0.05}_{-0.06}$	$46.20^{+0.05}_{-0.08}$	$45.44^{+0.07}_{-0.08}$	$44.93^{+0.05}_{-0.06}$
Q0121-590	$45.68^{+0.13}_{-0.12}$	$45.86^{+0.13}_{-0.11}$	$45.37^{+0.11}_{-0.10}$	$44.95^{+0.12}_{-0.12}$
Q0134+329	$46.80^{+0.07}_{-0.12}$	$46.92^{+0.08}_{-0.18}$	$45.92^{+0.13}_{-0.11}$	$45.47^{+0.07}_{-0.06}$
Q0205+024	$45.98^{+0.07}_{-0.08}$	$46.18^{+0.07}_{-0.08}$	$45.72^{+0.07}_{-0.08}$	$45.30^{+0.06}_{-0.07}$
Q0312-770	$46.03^{+0.26}_{-0.25}$	$46.25^{+0.28}_{-0.21}$	$45.77^{+0.22}_{-0.15}$	$45.49^{+0.20}_{-0.15}$
Q0414-060	$46.94^{+0.41}_{-0.13}$	$47.26^{+0.36}_{-0.09}$	$46.94^{+0.29}_{-0.06}$	$46.38^{+0.22}_{-0.08}$
Q0637-752	$47.38^{+0.06}_{-0.06}$	$47.55^{+0.16}_{-0.19}$	$46.93^{+0.37}_{-0.44}$	$46.56^{+0.23}_{-0.44}$
Q0804+761	$46.03^{+0.09}_{-0.10}$	$46.16^{+0.14}_{-0.13}$	$45.55^{+0.24}_{-0.22}$	$45.15^{+0.24}_{-0.23}$
Q0837-120	$45.90^{+0.11}_{-0.34}$	$46.18^{+0.10}_{-0.21}$	$45.82^{+0.08}_{-0.07}$	$45.31^{+0.06}_{-0.05}$
Q0844+349	$45.43^{+0.11}_{-0.15}$	$45.49^{+0.14}_{-0.14}$	$44.60^{+0.19}_{-0.13}$	$44.31^{+0.16}_{-0.11}$
Q0915+165	$45.01^{+0.11}_{-0.07}$	$45.05^{+0.12}_{-0.16}$	$43.92^{+0.12}_{-0.10}$	$43.42^{+0.11}_{-0.09}$
Q0923+129	$44.83^{+0.12}_{-0.12}$	$45.31^{+0.20}_{-0.48}$	$44.29^{+0.15}_{-0.14}$	$43.87^{+0.16}_{-0.15}$
Q1028+313	$45.74^{+0.35}_{-0.25}$	$46.05^{+0.25}_{-0.16}$	$45.73^{+0.06}_{-0.07}$	$45.28^{+0.05}_{-0.06}$
Q1100+772	$46.33^{+0.09}_{-0.08}$	$46.46^{+0.11}_{-0.11}$	$45.86^{+0.15}_{-0.18}$	$45.33^{+0.11}_{-0.15}$
Q1116+215	$46.42^{+0.06}_{-0.08}$	$46.58^{+0.07}_{-0.08}$	$46.01^{+0.08}_{-0.06}$	$45.75^{+0.06}_{-0.05}$
Q1137+660	$46.85^{+0.26}_{-0.18}$	$47.12^{+0.22}_{-0.14}$	$46.74^{+0.13}_{-0.09}$	$46.34^{+0.11}_{-0.09}$
Q1146-037	$45.69^{+0.98}_{-0.26}$	$45.97^{+0.82}_{-0.24}$	$45.62^{+0.26}_{-0.19}$	$44.92^{+0.35}_{-0.29}$
Q1202+281	$45.93^{+0.16}_{-0.18}$	$46.11^{+0.17}_{-0.21}$	$45.55^{+0.15}_{-0.20}$	$45.03^{+0.17}_{-0.21}$
Q1211+143	$45.98^{+0.07}_{-0.07}$	$46.26^{+0.11}_{-0.09}$	$45.92^{+0.15}_{-0.11}$	$45.34^{+0.13}_{-0.10}$
Q1219+755	$45.19^{+0.31}_{-0.23}$	$45.45^{+0.30}_{-0.16}$	$45.07^{+0.08}_{-0.09}$	$44.50^{+0.10}_{-0.10}$
Q1226+023	$47.08^{+0.06}_{-0.06}$	$47.28^{+0.07}_{-0.07}$	$46.70^{+0.08}_{-0.09}$	$46.28^{+0.08}_{-0.08}$
Q1244+026	$44.65^{+0.12}_{-0.09}$	$44.85^{+0.25}_{-0.16}$	$44.37^{+0.42}_{-0.16}$	$43.86^{+0.31}_{-0.11}$
Q1307+085	$45.98^{+0.07}_{-0.11}$	$46.13^{+0.12}_{-0.07}$	$45.63^{+0.12}_{-0.05}$	$45.22^{+0.09}_{-0.04}$
Q1351+695	$44.87^{+0.15}_{-0.12}$	$45.09^{+0.15}_{-0.18}$	$44.53^{+0.14}_{-0.16}$	$43.92^{+0.18}_{-0.20}$
Q1352+183	$45.87^{+0.14}_{-0.26}$	$45.94^{+0.30}_{-0.10}$	$45.59^{+0.22}_{-0.17}$	$45.19^{+0.15}_{-0.12}$
Q1407+265	$47.38^{+0.15}_{-0.18}$	$47.58^{+0.19}_{-0.14}$	$47.11^{+0.24}_{-0.07}$	$46.71^{+0.13}_{-0.06}$

TABLE 19—*Continued*

Name	UVOIR (0.1 – 100μm)	Bolometric (1 m-10 keV)	Ly cont (912Å-10 keV)	Ionizing Photon Rate
Q1416-129	$45.50^{+0.43}_{-0.23}$	$45.82^{+0.35}_{-0.20}$	$45.51^{+0.24}_{-0.18}$	$44.93^{+0.18}_{-0.17}$
Q1426+015	$45.86^{+0.11}_{-0.17}$	$46.07^{+0.15}_{-0.30}$	$45.60^{+0.22}_{-0.68}$	< 45.42
Q1501+106	$45.13^{+0.11}_{-0.11}$	$45.35^{+0.09}_{-0.09}$	$44.92^{+0.05}_{-0.06}$	$44.41^{+0.05}_{-0.06}$
Q1545+210	$46.27^{+0.10}_{-0.10}$	$46.47^{+0.12}_{-0.15}$	$46.00^{+0.16}_{-0.19}$	$45.57^{+0.13}_{-0.16}$
Q1613+658	$46.04^{+0.06}_{-0.08}$	$46.18^{+0.09}_{-0.19}$	$45.50^{+0.18}_{-0.72}$	< 45.23
Q1635+119	$45.33^{+0.55}_{-0.26}$	$45.50^{+0.67}_{-0.32}$	$44.98^{+0.76}_{-0.46}$	$44.59^{+0.69}_{-0.50}$
Q1704+608	$46.75^{+0.06}_{-0.07}$	$46.84^{+0.09}_{-0.08}$	$45.99^{+0.15}_{-0.11}$	$45.76^{+0.11}_{-0.09}$
Q1721+343	$46.31^{+0.10}_{-0.08}$	$46.51^{+0.14}_{-0.11}$	$46.03^{+0.13}_{-0.09}$	$45.56^{+0.12}_{-0.10}$
Q1803+676	$45.86^{+0.03}_{-0.32}$	$45.71^{+0.21}_{-0.09}$	$44.96^{+0.15}_{-0.13}$	$44.62^{+0.12}_{-0.11}$
Q2128-123	$46.87^{+0.14}_{-0.20}$	$47.01^{+0.15}_{-0.38}$	$46.02^{+0.34}_{-0.28}$	$45.44^{+0.37}_{-0.33}$
Q2130+099	$45.61^{+0.08}_{-0.08}$	$45.75^{+0.08}_{-0.09}$	$45.14^{+0.09}_{-0.10}$	$44.76^{+0.09}_{-0.10}$
Q2135-147	$46.16^{+0.09}_{-0.11}$	$46.32^{+0.14}_{-0.19}$	$45.73^{+0.18}_{-0.36}$	< 45.32
Q2209+184	$45.08^{+0.12}_{-0.11}$	$45.32^{+0.15}_{-0.19}$	$44.81^{+0.23}_{-0.22}$	$44.35^{+0.21}_{-0.21}$
Q2251-178	$45.59^{+0.09}_{-0.08}$	$45.75^{+0.13}_{-0.12}$	$45.19^{+0.20}_{-0.18}$	$44.70^{+0.20}_{-0.19}$

NOTE.—Values are logarithm of luminosity in units of erg s^{-1}; the 'ionizing photon rate' is the number of photons emitted per unit time, multiplied by 1 Rydberg to give it the units of luminosity.

TABLE 20
DECADE LUMINOSITIES

Name	(10-100 μm)	(1-10 μm)	(0.1-1μm)	(0.1-1 keV)	(1-10 keV)
Q0003+158	< 46.20	$45.77^{+0.37}_{-0.38}$	$46.58^{+0.08}_{-0.07}$	$46.83^{+2.41}_{-1.00}$	$45.52^{+0.87}_{-0.39}$
Q0003+199	$44.39^{+0.06}_{-0.11}$	$44.67^{+0.07}_{-0.08}$	$45.02^{+0.02}_{-0.02}$	$44.66^{+0.00}_{-0.00}$	$43.77^{+0.05}_{-0.04}$
Q0007+106	$45.11^{+0.05}_{-0.05}$	$45.24^{+0.08}_{-0.09}$	$45.41^{+0.03}_{-0.04}$	$44.30^{+0.54}_{-0.18}$	$44.97^{+0.08}_{-0.07}$
Q0026+129	< 45.02	$45.39^{+0.14}_{-0.13}$	$45.73^{+0.07}_{-0.06}$	$44.79^{+0.01}_{-0.01}$	$44.92^{+0.05}_{-0.04}$
Q0049+171	< 44.77	$43.98^{+0.49}_{-0.09}$	$44.62^{+0.06}_{-0.05}$	$44.52^{+2.01}_{-0.35}$	$44.37^{+0.20}_{-0.14}$
Q0050+124	$45.67^{+0.01}_{-0.01}$	$45.54^{+0.06}_{-0.06}$	$45.27^{+0.03}_{-0.03}$	$45.07^{+1.25}_{-0.53}$	–
Q0052+251	$45.40^{+0.08}_{-0.09}$	$45.38^{+0.08}_{-0.09}$	$45.83^{+0.06}_{-0.06}$	$45.12^{+1.18}_{-0.37}$	$44.89^{+0.25}_{-0.16}$
Q0054+144	$45.66^{+0.03}_{-0.08}$	$45.63^{+0.06}_{-0.06}$	$45.56^{+0.05}_{-0.05}$	$44.24^{+0.04}_{-0.04}$	$44.82^{+0.09}_{-0.09}$
Q0121-590	$45.05^{+0.01}_{-0.02}$	$45.08^{+0.18}_{-0.17}$	$45.39^{+0.16}_{-0.15}$	$44.61^{+0.09}_{-0.07}$	$44.43^{+0.06}_{-0.06}$
Q0134+329	$46.61^{+0.02}_{-0.09}$	$46.04^{+0.19}_{-0.31}$	$46.04^{+0.12}_{-0.11}$	$45.09^{+0.26}_{-0.24}$	–
Q0205+024	$45.35^{+0.09}_{-0.13}$	$45.37^{+0.06}_{-0.06}$	$45.69^{+0.06}_{-0.06}$	$44.55^{+0.05}_{-0.05}$	–
Q0312-770	< 45.56	$45.21^{+0.36}_{-0.98}$	$45.93^{+0.16}_{-0.16}$	$44.35^{+0.39}_{-0.12}$	–
Q0414-060	< 46.86	$46.14^{+0.71}_{-0.62}$	$46.84^{+0.05}_{-0.05}$	$45.43^{+1.23}_{-0.21}$	$46.63^{+0.07}_{-0.02}$
Q0637-752	$46.77^{+0.09}_{-0.24}$	$46.82^{+0.05}_{-0.05}$	$47.05^{+0.05}_{-0.05}$	$45.88^{+0.22}_{--}$	$46.24^{+0.11}_{-0.13}$
Q0804+761	$45.33^{+0.09}_{-0.08}$	$45.53^{+0.08}_{-0.09}$	$45.71^{+0.10}_{-0.10}$	$44.71^{+0.31}_{-0.26}$	$44.69^{+0.14}_{-0.13}$
Q0837-120	$45.20^{+0.11}_{-0.81}$	$45.40^{+0.14}_{-0.11}$	$45.59^{+0.10}_{-0.12}$	$45.06^{+0.16}_{-0.13}$	$45.22^{+0.05}_{-0.05}$
Q0844+349	$44.80^{+0.10}_{-0.18}$	$44.73^{+0.17}_{-0.22}$	$45.18^{+0.10}_{-0.12}$	$43.47^{+0.33}_{-0.15}$	–
Q0915+165	$44.62^{+0.04}_{-0.20}$	$44.64^{+0.07}_{-0.08}$	$44.20^{+0.33}_{-0.27}$	$43.12^{+0.14}_{-0.10}$	–
Q0923+129	$44.42^{+0.07}_{-0.09}$	$44.10^{+0.11}_{-0.14}$	$44.47^{+0.17}_{-0.14}$	$43.29^{+0.23}_{-0.19}$	$43.69^{+0.08}_{-0.08}$
Q1028+313	< 45.64	$45.16^{+0.41}_{-0.18}$	$45.55^{+0.08}_{-0.10}$	$44.52^{+0.04}_{-0.04}$	$44.97^{+0.05}_{-0.05}$
Q1100+772	$45.59^{+0.09}_{-0.14}$	$45.87^{+0.17}_{-0.16}$	$46.00^{+0.03}_{-0.03}$	$45.26^{+0.20}_{-0.31}$	–
Q1116+215	< 45.47	$45.89^{+0.06}_{-0.08}$	$46.23^{+0.05}_{-0.04}$	$44.74^{+0.19}_{-0.12}$	–
Q1137+660	< 46.46	$46.12^{+0.35}_{-0.44}$	$46.73^{+0.12}_{-0.10}$	$45.73^{+0.28}_{-0.07}$	$45.88^{+0.07}_{-0.11}$
Q1146-037	< 46.49	< 46.01	$45.60^{+0.18}_{-0.17}$	$44.86^{+0.30}_{-0.12}$	–
Q1202+281	$45.56^{+0.18}_{-0.24}$	$45.42^{+0.19}_{-0.19}$	$45.36^{+0.10}_{-0.09}$	$44.98^{+0.13}_{-0.24}$	–
Q1211+143	$45.41^{+0.08}_{-0.10}$	$45.41^{+0.06}_{-0.06}$	$45.64^{+0.07}_{-0.07}$	$45.62^{+0.22}_{-0.14}$	$44.71^{+0.08}_{-0.07}$
Q1219+755	< 45.00	$44.77^{+0.23}_{-0.20}$	$44.90^{+0.18}_{-0.15}$	$44.28^{+0.02}_{-0.02}$	$44.41^{+0.07}_{-0.10}$
Q1226+023	$46.44^{+0.05}_{-0.05}$	$46.48^{+0.07}_{-0.07}$	$46.79^{+0.07}_{-0.06}$	$45.48^{+0.02}_{-0.02}$	$46.02^{+0.10}_{-0.16}$
Q1244+026	$44.32^{+0.11}_{-0.09}$	$43.79^{+0.19}_{-0.12}$	$44.24^{+0.11}_{-0.06}$	$43.87^{+0.75}_{-0.24}$	–
Q1307+085	$45.32^{+0.12}_{-0.30}$	$45.29^{+0.09}_{-0.13}$	$45.73^{+0.05}_{-0.05}$	$44.64^{+0.30}_{-0.11}$	$44.92^{+0.03}_{-0.03}$
Q1351+695	$44.59^{+0.00}_{-0.01}$	$44.26^{+0.23}_{-0.33}$	$44.23^{+0.30}_{-0.23}$	$43.99^{+0.12}_{-0.16}$	$43.90^{+0.08}_{-0.08}$
Q1352+183	< 45.50	$45.22^{+0.21}_{-0.06}$	$45.59^{+0.04}_{-0.04}$	$44.86^{+0.50}_{-0.38}$	$44.45^{+0.04}_{-0.05}$
Q1407+265	$46.76^{+0.31}_{-0.78}$	$46.85^{+0.14}_{-0.16}$	$47.04^{+0.04}_{-0.04}$	$46.27^{+0.76}_{-0.15}$	$46.08^{+0.12}_{-0.06}$

TABLE 20--*Continued*

Name	(10-100 μm)	(1-10 μm)	(0.1-1μm)	(0.1-1 keV)	(1-10 keV)
Q1416-129	< 45.42	$44.75^{+0.57}_{-0.22}$	$45.41^{+0.18}_{-0.17}$	$44.90^{+0.37}_{-0.30}$	$44.88^{+0.17}_{-0.07}$
Q1426+015	$45.19^{+0.10}_{-0.17}$	$45.18^{+0.14}_{-0.21}$	$45.63^{+0.09}_{-0.15}$	$44.83^{+0.00}_{--}$	$44.70^{+0.04}_{-0.04}$
Q1501+106	$44.68^{+0.10}_{-0.12}$	$44.54^{+0.12}_{-0.12}$	$44.72^{+0.11}_{-0.10}$	$44.03^{+0.03}_{-0.03}$	$44.15^{+0.03}_{-0.03}$
Q1545+210	$45.49^{+0.06}_{-0.19}$	$45.64^{+0.07}_{-0.10}$	$46.05^{+0.11}_{-0.10}$	$45.20^{+0.20}_{-0.30}$	–
Q1613+658	$45.69^{+0.02}_{-0.05}$	$45.42^{+0.14}_{-0.16}$	$45.54^{+0.05}_{-0.07}$	$44.83^{+0.02}_{--}$	–
Q1635+119	< 45.47	$44.59^{+0.48}_{-0.05}$	$45.22^{+0.31}_{-0.24}$	$44.12^{+1.09}_{-0.32}$	–
Q1704+608	$46.27^{+0.07}_{-0.11}$	$46.24^{+0.07}_{-0.07}$	$46.32^{+0.03}_{-0.03}$	$44.41^{+0.37}_{-0.23}$	–
Q1721+343	$45.70^{+0.19}_{-0.10}$	$45.56^{+0.08}_{-0.11}$	$46.07^{+0.06}_{-0.07}$	$45.06^{+0.24}_{-0.16}$	$45.47^{+0.06}_{-0.04}$
Q1803+676	< 44.94	$45.28^{+0.01}_{-0.05}$	$45.50^{+0.09}_{-0.08}$	$43.65^{+0.24}_{-0.15}$	–
Q2128-123	$46.43^{+0.14}_{-0.19}$	$46.09^{+0.23}_{-0.85}$	$46.53^{+0.10}_{-0.10}$	$45.24^{+0.46}_{-0.25}$	$45.51^{+0.21}_{-0.23}$
Q2130+099	$45.10^{+0.04}_{-0.05}$	$45.09^{+0.11}_{-0.11}$	$45.20^{+0.08}_{-0.08}$	$43.75^{+0.05}_{-0.05}$	$44.04^{+0.07}_{-0.05}$
Q2135-147	$45.66^{+0.13}_{-0.19}$	$45.57^{+0.10}_{-0.12}$	$45.79^{+0.04}_{-0.05}$	$44.94^{+0.07}_{--}$	$45.34^{+0.07}_{-0.10}$
Q2209+184	$44.39^{+0.02}_{-0.02}$	$44.27^{+0.21}_{-0.21}$	$44.89^{+0.12}_{-0.12}$	$44.10^{+0.29}_{-0.26}$	–
Q2251-178	$44.89^{+0.10}_{-0.05}$	$44.98^{+0.07}_{-0.08}$	$45.34^{+0.09}_{-0.09}$	$44.29^{+0.35}_{-0.33}$	$44.69^{+0.09}_{-0.07}$

NOTE.—Values are logarithm of luminosity in units of erg s^{-1}

TABLE 21
OCTAVE LUMINOSITIES

Name	(0.8-1.6 μm)	(0.4-0.8 μm)	(0.2-0.4 μm)	(0.1-0.2 μm)	(0.15-0.3 keV)	(1-2 keV)
Q0003+158	$45.47^{+0.07}_{-0.09}$	$45.77^{+0.03}_{-0.03}$	$46.16^{+0.05}_{-0.05}$	$46.20^{+0.11}_{-0.11}$	$46.40^{+2.26}_{-1.05}$	$45.41^{+0.81}_{-0.34}$
Q0003+199	$44.02^{+0.06}_{-0.06}$	$44.15^{+0.04}_{-0.04}$	$44.58^{+0.02}_{-0.02}$	$44.69^{+0.02}_{-0.02}$	$44.23^{+0.00}_{-0.00}$	$43.40^{+0.03}_{-0.04}$
Q0007+106	$44.47^{+0.10}_{-0.13}$	$44.64^{+0.03}_{-0.04}$	$44.97^{+0.03}_{-0.03}$	$45.04^{+0.04}_{-0.04}$	$43.65^{+0.63}_{-0.21}$	$44.14^{+0.25}_{-0.19}$
Q0026+129	$44.87^{+0.09}_{-0.08}$	$45.01^{+0.02}_{-0.02}$	$45.24^{+0.03}_{-0.03}$	$45.36^{+0.12}_{-0.12}$	$44.25^{+0.03}_{-0.03}$	$44.35^{+0.01}_{-0.01}$
Q0049+171	$43.60^{+0.17}_{-0.16}$	$43.86^{+0.02}_{-0.02}$	$44.22^{+0.04}_{-0.04}$	$44.20^{+0.09}_{-0.06}$	$44.03^{+2.00}_{-0.42}$	$43.87^{+0.40}_{-0.37}$
Q0050+124	$44.77^{+0.06}_{-0.07}$	$44.75^{+0.02}_{-0.02}$	$44.83^{+0.03}_{-0.03}$	$44.65^{+0.04}_{-0.04}$	$44.63^{+1.21}_{-0.57}$	$43.89^{+0.45}_{-0.33}$
Q0052+251	$44.70^{+0.08}_{-0.12}$	$44.90^{+0.02}_{-0.04}$	$45.31^{+0.04}_{-0.04}$	$45.58^{+0.08}_{-0.07}$	$44.63^{+1.24}_{-0.43}$	$44.46^{+0.42}_{-0.26}$
Q0054+144	$44.88^{+0.04}_{-0.04}$	$45.01^{+0.02}_{-0.02}$	$45.15^{+0.05}_{-0.05}$	$44.95^{+0.08}_{-0.07}$	$43.57^{+0.05}_{-0.05}$	$44.12^{+0.03}_{-0.03}$
Q0121-590	$44.09^{+0.43}_{-0.62}$	$44.38^{+0.27}_{-0.27}$	$44.93^{+0.16}_{-0.16}$	$45.13^{+0.13}_{-0.13}$	$44.07^{+0.10}_{-0.09}$	$44.14^{+0.04}_{-0.04}$
Q0134+329	$45.02^{+0.24}_{-0.33}$	$45.26^{+0.06}_{-0.07}$	$45.57^{+0.06}_{-0.06}$	$45.71^{+0.18}_{-0.16}$	$44.51^{+0.31}_{-0.31}$	$44.76^{+0.12}_{-0.11}$
Q0205+024	$44.57^{+0.09}_{-0.10}$	$44.87^{+0.04}_{-0.04}$	$45.26^{+0.06}_{-0.06}$	$45.34^{+0.07}_{-0.06}$	$44.11^{+0.05}_{-0.05}$	$44.01^{+0.04}_{-0.05}$
Q0312-770	$44.76^{+0.16}_{-0.38}$	$45.12^{+0.08}_{-0.13}$	$45.28^{+0.16}_{-0.14}$	$45.70^{+0.18}_{-0.17}$	$43.61^{+0.42}_{-0.14}$	$44.35^{+0.31}_{-0.13}$
Q0414-060	$45.77^{+0.18}_{-0.22}$	$46.01^{+0.07}_{-0.07}$	$46.27^{+0.05}_{-0.04}$	$46.58^{+0.05}_{-0.05}$	$44.80^{+1.40}_{-0.22}$	$45.22^{+0.63}_{-0.17}$
Q0637-752	$46.23^{+0.02}_{-0.02}$	$46.33^{+0.05}_{-0.05}$	$46.46^{+0.09}_{-0.09}$	$46.76^{+0.04}_{-0.04}$	< 44.96	$45.54^{+0.03}_{-0.05}$
Q0804+761	$44.70^{+0.13}_{-0.25}$	$44.88^{+0.08}_{-0.13}$	$45.31^{+0.03}_{-0.03}$	$45.34^{+0.17}_{-0.16}$	$44.19^{+0.36}_{-0.32}$	$44.18^{+0.11}_{-0.12}$
Q0837-120	$44.63^{+0.27}_{-0.74}$	$44.69^{+0.15}_{-0.28}$	$45.07^{+0.10}_{-0.11}$	$45.33^{+0.08}_{-0.08}$	$44.47^{+0.20}_{-0.17}$	$44.76^{+0.07}_{-0.06}$
Q0844+349	$44.10^{+0.32}_{-1.00}$	$44.47^{+0.18}_{-0.29}$	$44.78^{+0.07}_{-0.07}$	$44.76^{+0.07}_{-0.06}$	$42.85^{+0.43}_{-0.23}$	$43.23^{+0.12}_{-0.10}$
Q0915+165	$43.61^{+0.35}_{-0.81}$	$43.59^{+0.61}_{-1.06}$	$43.78^{+0.16}_{-0.18}$	$43.66^{+0.06}_{-0.06}$	$42.45^{+0.20}_{-0.16}$	$42.99^{+0.07}_{-0.07}$
Q0923+129	$43.17^{+0.34}_{-0.65}$	$43.33^{+0.59}_{-0.95}$	$43.93^{+0.11}_{-0.13}$	$44.26^{+0.10}_{-0.10}$	$42.71^{+0.29}_{-0.25}$	$42.96^{+0.09}_{-0.10}$
Q1028+313	$44.59^{+0.19}_{-0.52}$	$44.73^{+0.11}_{-0.19}$	$44.99^{+0.09}_{-0.09}$	$45.27^{+0.06}_{-0.06}$	$43.93^{+0.04}_{-0.04}$	$44.30^{+0.04}_{-0.04}$
Q1100+772	$45.27^{+0.08}_{-0.08}$	$45.46^{+0.02}_{-0.02}$	$45.63^{+0.02}_{-0.02}$	$45.31^{+0.06}_{-0.06}$	$44.74^{+0.22}_{-0.38}$	$44.74^{+0.13}_{-0.11}$
Q1116+215	$45.20^{+0.07}_{-0.07}$	$45.39^{+0.03}_{-0.04}$	$45.74^{+0.03}_{-0.02}$	$45.93^{+0.06}_{-0.06}$	$44.22^{+0.22}_{-0.15}$	$44.22^{+0.08}_{-0.06}$
Q1137+660	$45.63^{+0.04}_{-0.05}$	$45.94^{+0.03}_{-0.03}$	$46.21^{+0.06}_{-0.05}$	$46.44^{+0.18}_{-0.17}$	$45.15^{+0.34}_{-0.08}$	$45.40^{+0.09}_{-0.05}$
Q1146-037	$44.31^{+0.36}_{-0.97}$	$44.63^{+0.23}_{-0.36}$	$45.22^{+0.16}_{-0.15}$	$45.26^{+0.18}_{-0.15}$	$44.18^{+0.37}_{-0.15}$	$44.75^{+0.17}_{-0.08}$
Q1202+281	$44.41^{+0.27}_{-0.37}$	$44.50^{+0.06}_{-0.06}$	$44.90^{+0.07}_{-0.07}$	$45.04^{+0.12}_{-0.12}$	$44.47^{+0.14}_{-0.29}$	$44.39^{+0.11}_{-0.11}$
Q1211+143	$44.76^{+0.06}_{-0.06}$	$44.96^{+0.06}_{-0.06}$	$45.22^{+0.06}_{-0.06}$	$45.21^{+0.08}_{-0.08}$	$45.19^{+0.22}_{-0.14}$	$44.37^{+0.06}_{-0.07}$
Q1219+755	$44.12^{+0.38}_{-0.37}$	$44.19^{+0.24}_{-0.17}$	$44.47^{+0.16}_{-0.14}$	$44.49^{+0.14}_{-0.14}$	$43.74^{+0.02}_{-0.02}$	$43.94^{+0.01}_{-0.01}$
Q1226+023	$45.87^{+0.05}_{-0.05}$	$46.03^{+0.03}_{-0.03}$	$46.33^{+0.05}_{-0.05}$	$46.44^{+0.09}_{-0.09}$	$44.85^{+0.02}_{-0.02}$	$45.33^{+0.01}_{-0.01}$
Q1244+026	$42.88^{+0.23}_{-0.20}$	$43.34^{+0.34}_{-0.22}$	$43.91^{+0.06}_{-0.04}$	$43.83^{+0.04}_{-0.03}$	$43.40^{+0.78}_{-0.28}$	$43.07^{+0.10}_{-0.18}$
Q1307+085	$44.74^{+0.14}_{-0.28}$	$45.01^{+0.09}_{-0.13}$	$45.23^{+0.04}_{-0.04}$	$45.39^{+0.02}_{-0.02}$	$44.10^{+0.37}_{-0.14}$	$44.19^{+0.06}_{-0.07}$
Q1351+695	$43.59^{+0.53}_{-1.00}$	$43.14^{+0.71}_{-0.27}$	$43.80^{+0.14}_{-0.17}$	$43.93^{+0.21}_{-0.24}$	$43.48^{+0.14}_{-0.21}$	$43.40^{+0.06}_{-0.05}$
Q1352+183	$44.56^{+0.11}_{-0.11}$	$44.83^{+0.01}_{-0.01}$	$45.13^{+0.04}_{-0.04}$	$45.23^{+0.05}_{-0.05}$	$44.40^{+0.52}_{-0.44}$	$43.99^{+0.08}_{-0.12}$
Q1407+265	$46.02^{+0.06}_{-0.06}$	$46.26^{+0.04}_{-0.04}$	$46.57^{+0.02}_{-0.02}$	$46.70^{+0.05}_{-0.05}$	$45.78^{+0.82}_{-0.17}$	$45.61^{+0.24}_{-0.07}$

TABLE 21—*Continued*

Name	(0.8-1.6 μm)	(0.4-0.8 μm)	(0.2-0.4 μm)	(0.1-0.2 μm)	(0.15-0.3 keV)	(1-2 keV)
Q1416-129	$44.21^{+0.45}_{-0.64}$	$44.45^{+0.29}_{-0.29}$	$45.01^{+0.15}_{-0.15}$	$45.07^{+0.16}_{-0.15}$	$44.36^{+0.35}_{-0.36}$	$44.45^{+0.33}_{-0.17}$
Q1426+015	$44.53^{+0.23}_{-0.64}$	$44.66^{+0.10}_{-0.18}$	$45.11^{+0.07}_{-0.07}$	$45.37^{+0.10}_{-0.18}$	$44.30^{+0.10}_{--}$	$44.20^{+0.04}_{-0.04}$
Q1501+106	$43.68^{+0.31}_{-0.44}$	$43.82^{+0.21}_{-0.21}$	$44.29^{+0.12}_{-0.12}$	$44.41^{+0.05}_{-0.05}$	$43.54^{+0.03}_{-0.03}$	$43.61^{+0.02}_{-0.02}$
Q1545+210	$44.99^{+0.08}_{-0.08}$	$45.27^{+0.04}_{-0.05}$	$45.58^{+0.10}_{-0.09}$	$45.72^{+0.15}_{-0.14}$	$44.64^{+0.22}_{-0.37}$	$44.81^{+0.16}_{-0.14}$
Q1613+658	$44.56^{+0.19}_{-0.24}$	$44.75^{+0.07}_{-0.08}$	$45.08^{+0.06}_{-0.06}$	$45.19^{+0.03}_{-0.07}$	$44.31^{+0.11}_{--}$	$44.22^{+0.05}_{-0.04}$
Q1635+119	$44.31^{+0.07}_{-0.07}$	$44.51^{+0.06}_{-0.06}$	$44.61^{+0.16}_{-0.15}$	$44.93^{+0.44}_{-0.43}$	$43.54^{+1.22}_{-0.43}$	$43.79^{+0.50}_{-0.27}$
Q1704+608	$45.51^{+0.06}_{-0.06}$	$45.64^{+0.02}_{-0.02}$	$45.82^{+0.03}_{-0.03}$	$45.95^{+0.02}_{-0.02}$	$43.75^{+0.46}_{-0.31}$	$44.25^{+0.16}_{-0.12}$
Q1721+343	$44.94^{+0.12}_{-0.21}$	$45.21^{+0.06}_{-0.08}$	$45.61^{+0.04}_{-0.04}$	$45.76^{+0.08}_{-0.08}$	$44.43^{+0.29}_{-0.22}$	$44.85^{+0.13}_{-0.07}$
Q1803+676	$44.64^{+0.04}_{-0.04}$	$44.76^{+0.03}_{-0.03}$	$45.06^{+0.06}_{-0.05}$	$45.12^{+0.15}_{-0.13}$	$42.81^{+0.28}_{-0.21}$	$43.80^{+0.20}_{-0.12}$
Q2128-123	$45.60^{+0.07}_{-0.14}$	$45.79^{+0.09}_{-0.10}$	$46.07^{+0.11}_{-0.11}$	$46.16^{+0.10}_{-0.10}$	$44.61^{+0.55}_{-0.31}$	$45.02^{+0.21}_{-0.14}$
Q2130+099	$44.12^{+0.27}_{-0.43}$	$44.34^{+0.05}_{-0.05}$	$44.74^{+0.03}_{-0.03}$	$44.89^{+0.12}_{-0.12}$	$43.24^{+0.05}_{-0.05}$	$43.42^{+0.03}_{-0.03}$
Q2135-147	$44.86^{+0.13}_{-0.13}$	$45.20^{+0.04}_{-0.04}$	$45.38^{+0.03}_{-0.03}$	$45.25^{+0.05}_{-0.09}$	$44.34^{+0.04}_{--}$	$44.56^{+0.02}_{-0.02}$
Q2209+184	$43.13^{+0.55}_{-0.37}$	$43.98^{+0.09}_{-0.12}$	$44.51^{+0.10}_{-0.09}$	$44.54^{+0.14}_{-0.14}$	$43.54^{+0.35}_{-0.35}$	$43.70^{+0.15}_{-0.14}$
Q2251-178	$44.38^{+0.06}_{-0.08}$	$44.63^{+0.04}_{-0.04}$	$44.83^{+0.09}_{-0.09}$	$44.97^{+0.11}_{-0.11}$	$43.64^{+0.42}_{-0.42}$	$44.13^{+0.21}_{-0.20}$

NOTE.—Values are logarithm of luminosity in units of erg s^{-1}

TABLE 22
BOLOMETRIC CORRECTIONS

	Median	Mean, Sigma	Min	Max
$L_{Bol}/L_{2500\AA}$	5.2	6.2±2.7	2.7	16.8
L_{Bol}/L_B	10.7	11.7±4.4	5.1	25.1
L_{Bol}/L_V	13.3	14.1±5.3	6.6	29.2
$L_{Bol}/L_{1.5\mu m}$	24.5	25.4±8.9	8.7	41.8
$L_{UVOIR}/L_{2500\AA}$	3.5	4.1±2.2	1.4	12.8
L_{UVOIR}/L_B	7.0	7.5±3.5	4.2	22.7
L_{UVOIR}/L_V	8.2	9.1±3.9	4.7	23.0
$L_{UVOIR}/L_{1.5\mu m}$	15.4	16.1±5.5	8.1	29.5
L_{Ion}/L_{Bol}	0.32	0.32±0.13	0.07	0.68
$N_{Ion}R/L_{Bol}$	0.11	0.11±0.04	0.02	0.19
$L_{Ion}/N_{Ion}R$	2.8	3.0±0.8	1.7	5.0

NOTE.— Bolometric correction factors for UV, visible and infrared monochromatic luminosities. Monochromatic luminosities are defined to be the value of $\nu L(\nu)$ in the rest frame. Mean and standard deviation are given, followed by the minimum and maximum values found in the sample. Errors in the determination of individual energy distributions have been ignored for the purposes of this table. Also listed are estimates of the ionizing flux discussed in the text.

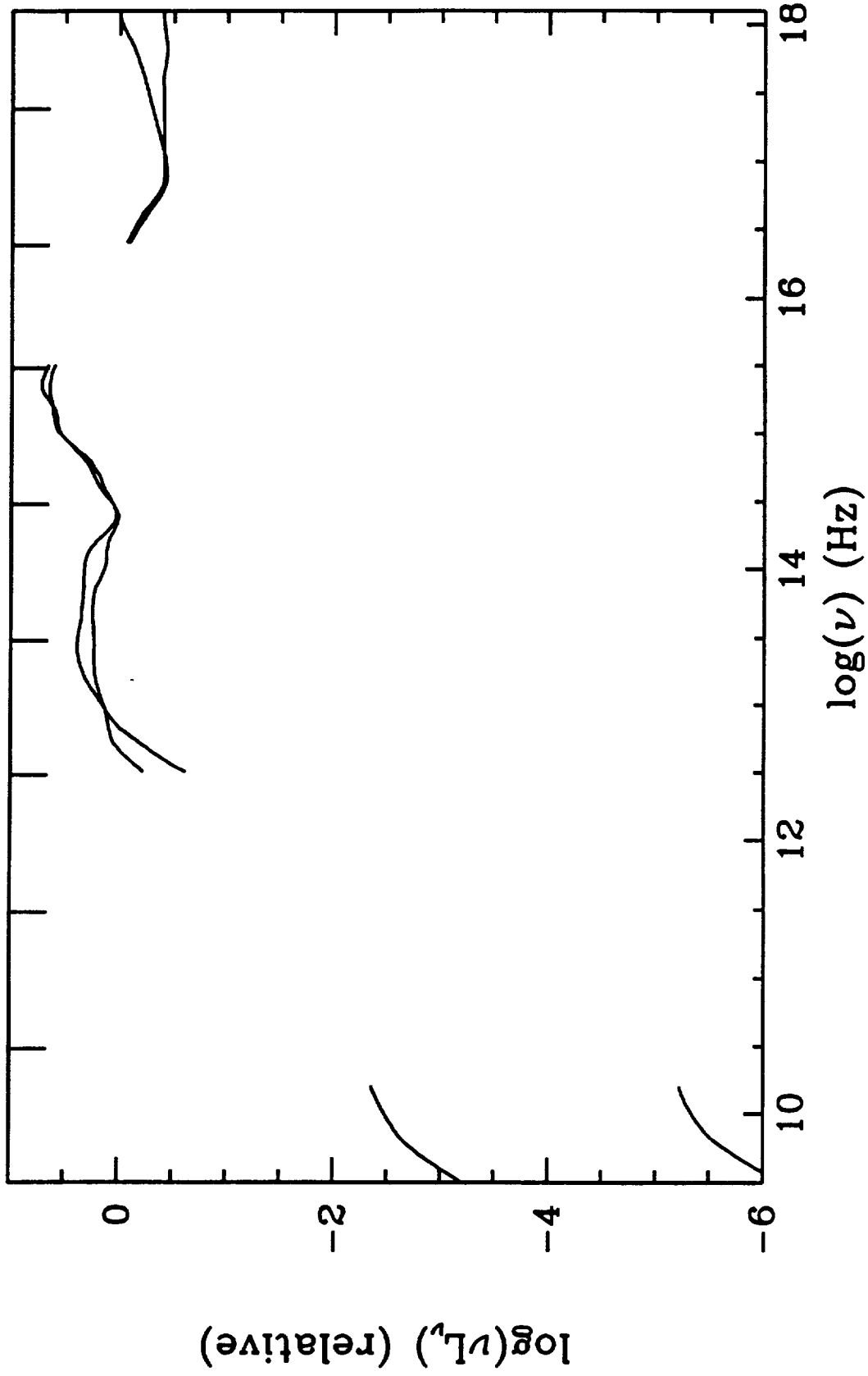

Fig. 55

Fig. 56

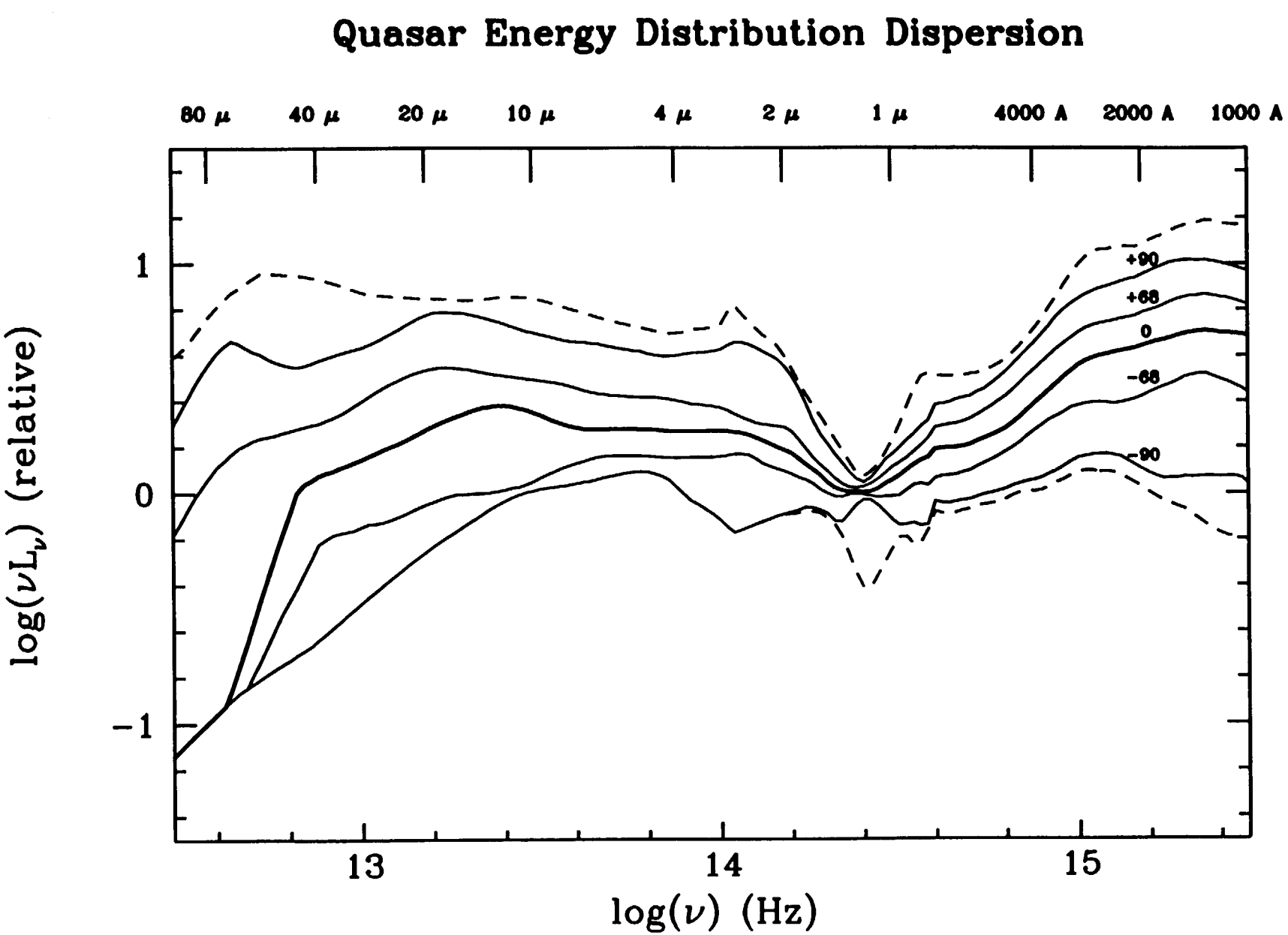
Quasar Energy Distribution Dispersion
80 μ
40 μ
20 μ
10 μ
4 μ
2 μ
1 μ
4000 A
2000 A
1000 A
+90
+68
0
-68
-90
1
0
−1
log(νL_ν) (relative)
13
14
15
log(ν) (Hz)